

# On the brightness distribution of Type Ia supernovae from violent white dwarf mergers

A. J. Ruiter<sup>1\*</sup>, S. A. Sim<sup>2</sup>, R. Pakmor<sup>3</sup>, M. Kromer<sup>1</sup>, I. R. Seitenzahl<sup>1,4</sup>, K. Belczynski<sup>5,6</sup>, M. Fink<sup>1,4</sup>, M. Herzog<sup>1</sup>, W. Hillebrandt<sup>1</sup>, F. K. Röpké<sup>1,4</sup>, S. Taubenberger<sup>1</sup>

<sup>1</sup>Max-Planck-Institut für Astrophysik, Karl-Schwarzschild- Str. 1, D-85741 Garching, Germany

<sup>2</sup>Research School of Astronomy and Astrophysics, The Australian National University, Mount Stromlo Observatory, Cotter Road, Weston Creek, ACT 2611, Australia

<sup>3</sup>Heidelberger Institut für Theoretische Studien, Schloss- Wolfsbrunnenweg 35, 69118 Heidelberg, Germany

<sup>4</sup>Institut für Theoretische Physik und Astrophysik, Universität Würzburg, Am Hubland, D-97074 Würzburg, Germany

<sup>5</sup>Astronomical Observatory, University of Warsaw, Al. Ujazdowskie 4, 00-478 Warsaw, Poland

<sup>6</sup>Center for Gravitational Wave Astronomy, University of Texas at Brownsville, Brownsville, TX 78520, USA

21 February 2022

## ABSTRACT

We investigate the brightness distribution expected for thermonuclear explosions that might result from the ignition of a detonation during the violent merger of white dwarf (WD) binaries. Violent WD mergers are a subclass of the canonical double degenerate scenario where two carbon-oxygen (CO) WDs merge when the larger WD fills its Roche-lobe. Determining their brightness distribution is critical for evaluating whether such an explosion model could be responsible for a significant fraction of the observed population of Type Ia supernovae (SNe Ia). We argue that the brightness of an explosion realised via the violent merger model is mainly determined by the mass of  $^{56}\text{Ni}$  produced in the detonation of the primary CO WD. To quantify this link, we use a set of sub-Chandrasekhar mass WD detonation models to derive a relationship between primary WD mass ( $m_{\text{WD}}$ ) and expected peak bolometric brightness ( $M_{\text{bol}}$ ). We use this  $m_{\text{WD}}-M_{\text{bol}}$  relationship to convert the masses of merging primary WDs from binary population models to a predicted distribution of explosion brightness. We also investigate the sensitivity of our results to assumptions about the conditions required to realise a detonation during violent mergers of WDs. We find a striking similarity between the shape of our theoretical peak-magnitude distribution and that observed for SNe Ia: our model produces a  $M_{\text{bol}}$  distribution that roughly covers the range and matches the shape of the one observed for SNe Ia. However, this agreement hinges on a particular phase of mass accretion during binary evolution: the primary WD gains  $\sim 0.15 - 0.35 M_{\odot}$  from a slightly-evolved helium star companion. In our standard binary evolution model, such an accretion phase is predicted to occur for about 43% of all binary systems that ultimately give rise to binary CO WD mergers. We also find that with high probability, violent WD mergers involving the most massive primaries ( $\gtrsim 1.3 M_{\odot}$ , which should produce bright SNe) have delay times  $\lesssim 500$  Myr.

**Key words:** hydrodynamics – radiative transfer – methods: numerical – binaries: close – supernovae: general – white dwarfs

## 1 INTRODUCTION

It is widely agreed that the progenitors of Type Ia supernovae (SNe Ia) are thermonuclear explosions of carbon-oxygen (CO) white dwarfs (WDs) in binary systems. However, it is still not clear whether their companion stars (secondaries) are hydrogen-rich (main sequence or giant stars, typically called ‘single degenerate’ scenarios), helium-rich (helium stars or helium-rich WDs) or

other CO WDs which merge with the primaries (typically called ‘double degenerate’ scenarios).

Sternberg et al. (2011) analysed high-resolution spectra of 35 SNe Ia, finding that more than half of the spectra exhibit a blueshifted Na I D absorption feature. The authors attribute this feature to circumstellar material (blown off of the secondary prior to the SN explosion), suggesting that at least 20% of SNe Ia in spiral galaxies originate from single degenerate scenarios (see also Patat et al. 2011). On the other hand, several recent studies have highlighted challenges to single degenerate scenarios and have instead tended to favour double degenerate models.

\* E-mail: ajr@mpa-garching.mpg.de

For example, the lack of emission associated with the supernova overrunning the companion star (Kasen 2010; Hayden et al. 2010; Ganeshalingam et al. 2011; Bianco et al. 2011), the absence of radio detections (Hancock et al. 2011; Chomiuk et al. 2012; Horesh et al. 2012) and the lack of unambiguous identifications of companion stars in supernova remnants (Ruiz-Lapuente et al. 2004; Kerzendorf et al. 2009) argue against models in which the companion is a red giant star at explosion (see also Bloom et al. 2012, where a single degenerate scenario origin for SN 2011fe is likely ruled out). In addition, a number of recent studies find that the delay time distribution (DTD) of SNe Ia follows a power-law shape  $t^s$ , where  $-1.6 \leq s \leq -1$  (Maoz et al. 2010; Graur et al. 2011; Barbary et al. 2012; Sand et al. 2012). Such a distribution is expected if the progenitor population of SNe Ia is dominated by double degenerates. These studies, among others, have fuelled speculation that there must be at least two different progenitor scenarios leading to SNe Ia. However, the question of which channel(s) dominate(s) the production of ‘normal’ SNe Ia (Benetti et al. 2005; Branch et al. 2009) and determine(s) the observed SN Ia brightness distribution remains open.

In a series of recent papers (Pakmor et al. 2010, 2011, 2012; Röpke et al. 2012), a new explosion model for SNe Ia produced by double degenerate (CO+CO WDs) mergers was investigated. In this violent merger model, a prompt detonation is triggered during the merger itself, leading to a thermonuclear explosion of the system. Although it is not yet established which parameters of the merging system are most crucial for the formation of such a detonation (see e.g., Dan et al. 2012), synthetic spectra and light-curves computed for several realisations of the violent merger scenario are a good match to maximum light observations of SNe Ia (Pakmor et al. 2010, 2012). The level of agreement with observations is comparable to that found for other scenarios (Röpke et al. 2012).

In contrast to Chandrasekhar mass explosion models, where the peak brightness is driven by stochastic processes connected to the formation of deflagration and detonation flames or other properties of the exploding Chandrasekhar mass WD (e.g. Kasen et al. 2009; Blondin et al. 2011; Seitenzahl et al. 2011), in the violent merger scenario there is a direct correlation between fundamental parameters of the progenitor system and the SN luminosity. Specifically, to first order, the violent merger model can be interpreted as a mechanism to ignite a detonation of a sub-Chandrasekhar-mass WD (the primary CO WD) as described in Sim et al. (2010) (see also Fink et al. 2010). Although the merging secondary WD is also consumed by the thermonuclear flame of the detonation, it does not produce any iron group elements when it is burned. Thus, the absolute brightness of a SN Ia explosion depends on the mass of the primary CO WD.

The brightness distribution of SNe Ia can be observed directly, with a typical peak brightness of  $\simeq -19$  mag (Richardson et al. 2002; Benetti et al. 2005) and a spread in brightness of  $\sim 1$  mag. Recently, Li et al. (2011) presented the brightness distribution of a volume-limited sample of SNe Ia. Any theoretical scenario explaining SNe Ia that claims to account for a large fraction of observed events must be able to reproduce the observed brightness distribution. The goal of this paper is to quantify the brightness distribution of SNe Ia from the violent merger scenario.

Our study requires three main inputs. First, we need predictions of the distribution of properties of merging CO+CO WD pairs. These we obtain from previously published STARTRACK (Belczynski et al. 2002, 2008) binary population synthesis models, which are described in Section 2. Second, we must consider which

characteristics of a merging system will be required for the explosion mechanism to work. This specification will be made based on the mass ratio of the merging system, as described in Section 3. Third, we need to estimate the brightness of an explosion based on the properties of the merging WDs. This is discussed in Section 4. In Section 5, we present our results based on the standard model used for the double degenerate scenario (DDS) in Ruiter et al. (2011) and comment on the comparison with observations. We discuss important implications and uncertainties of our modelling in Section 6 before drawing conclusions in Section 7.

## 2 BINARY POPULATION SYNTHESIS

### 2.1 Mass exchange for StarTrack binaries

We consider the population synthesis calculation results from the standard model of Ruiter et al. (2011), whose data were obtained with the STARTRACK population synthesis binary evolution code. In this subsection, we briefly explain how stellar mass loss/gain is handled over the course of binary evolution in STARTRACK.

*Unstable mass transfer.* Outside densely populated environments – such as the cores of globular clusters – binary stars that form close double WDs must undergo at least one common envelope (CE) phase (Iben & Livio 1993), in which the size of the binary orbit decreases (often significantly) upon expulsion of the mass-losing star’s envelope. Currently, CE ejection remains a poorly understood process in astrophysics. Observationally, it is difficult to study since it is a short-lived evolutionary phase<sup>1</sup> and detailed theoretical modelling is extremely challenging given the large spatial and temporal scales that must be taken into account to properly approach the problem (Ricker & Taam 2012). However, despite our collective ignorance, the CE phase cannot be ignored in binary evolution modelling, and so a simplified parametrization of the CE phase is often employed in binary population synthesis codes.

In the standard model of Ruiter et al. (2011), the CE parametrization  $\alpha_{\text{CE}}\lambda = 1$  was used. In this CE parametrization, often coined the ‘energy formalism’ (Webbink 1984), it is assumed that the binary can expel the envelope without merging if the binding energy of the mass-losing star’s envelope is not greater than the orbital energy of the binary with some efficiency factor  $\alpha_{\text{CE}}$ ;  $\Delta E_{\text{bin}} \leq \alpha_{\text{CE}} \Delta E_{\text{orb}}$  (but see also Ivanova & Chaichenets 2011; Ivanova 2011, for an overview and recent work on the CE problem). Since our calculations are based on the results of Ruiter et al. (2011), we assume as they do that the transfer of energy from the orbit to the removal of the envelope during CE is fully efficient, and thus  $\alpha_{\text{CE}} = 1$ . The binding energy is inversely proportional to the term  $\lambda$ , which is a parametrization of the structure of the mass-losing star (e.g. de Kool 1990).  $\lambda$  is somewhat uncertain, but is often assumed to be on the order of unity in population synthesis calculations for low- and intermediate-mass stars on the main sequence (MS) or the giant branch (Dewi & Tauris 2000). We take the CE parametrization with  $\alpha_{\text{CE}} = 1$  and  $\lambda = 1$  from Ruiter et al. (2011) for the current study.

*Stable mass transfer.* For Roche-lobe overflow (RLOF) on to non-degenerate accretors, mass transfer is assumed to be non-conservative. An efficiency parameter – which characterizes the fraction of matter transferred to the companion – is adopted (termed

<sup>1</sup> Though the sample of post-CE binaries (PCEBs) is becoming larger (Zorotovic et al. 2011).

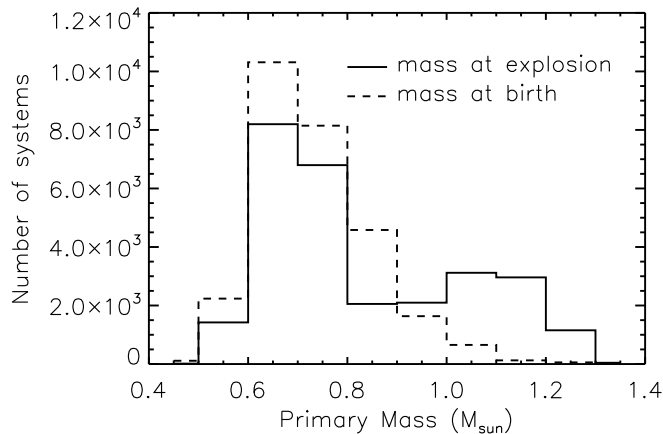


**Figure 1.** The mass distribution of the primary WD for all CO+CO WD binaries at the time of the merger from the Ruiter et al. (2011) standard calculation (solid histogram). The dashed histogram shows the mass distribution of the primary when it becomes a CO WD (i.e. neglecting any mass accretion which may occur after the primary WD has formed, see text). The numbers on the  $y$ -axis are not scaled, and show the actual numbers of CO+CO WD mergers produced in a Hubble time in the simulation of  $4.5 \times 10^6$  zero-age main sequence binary stars.

$f_a$  in Equation (33) of Belczynski et al. 2008). In Ruiter et al. (2011),  $f_a = 0.5$  was adopted for the standard calculations (see also Mennekens et al. 2010, where the same parameter is termed ‘ $\beta$ ’). Thus only 50% of the matter lost by the donor is gained by the accretor (Eddington-limited) while the rest is lost from the binary system with the specific angular momentum of the orbit (see Appendix A for more discussion).

For WD accretors, the STARTRACK code takes into account a number of published results on mass accretion on to CO WDs for hydrogen-rich accretion (Priyalnik & Kovetz 1995; Nomoto et al. 2007), and helium-rich accretion (Kato & Hachisu 1999, 2004, see also Taam 1980; García-Senz et al. 1999). In this case, the fraction of mass gained by the accretor is dependent upon the rate at which mass is transferred from the donor and the mass of the accreting WD. Mass that is lost from the binary carries with it the specific angular momentum of the accretor. A more detailed description can be found in Belczynski et al. (2008, section 5.7.2).

## 2.2 Primary mass distribution

Fig. 1 shows the distribution of primary (more massive WD) masses for merging CO+CO WD pairs at the time of merger from the Ruiter et al. (2011)  $\alpha_{CE\lambda} = 1$  calculation (solid histogram). Note that this  $m_{WD}$  distribution has two peaks: a prominent peak at  $\sim 0.65 M_{\odot}$  and a smaller bump at  $\sim 1.1 M_{\odot}$ . For comparison, we show the distribution of primary masses for the same population of merging CO+CO WD pairs recorded at the time of primary WD birth (dashed histogram); this distribution has only a single peak at  $\sim 0.65 M_{\odot}$ . This ‘mass shift’ to larger masses is the result of a phase of mass accretion when the donor star is in the helium-burning phase, which we discuss in detail in Section 2.3. As we will discuss in Section 4, this has important implications for our predicted brightness distribution of SNe Ia.

## 2.3 Binary evolution and example

To understand the origin of the double-peaked  $m_{WD}$ -distribution, we have analysed various binary evolution histories for representative systems in the STARTRACK simulations. The formation of the secondary bump at  $\sim 1.1 M_{\odot}$  in the solid histogram of Fig. 1 (and more generally the larger average primary WD masses) is associated with CO WD primaries that accreted material from a slightly evolved naked helium star companion ( $k=8$  in Hurley et al. 2000).

To be more specific, we present a typical evolutionary channel along with the relevant physical processes that may potentially lead to the formation of a CO+CO WD merger that contributes to the bump at  $\sim 1.1 M_{\odot}$  in Fig. 1. In our example, the initially more massive star on the zero-age main sequence (ZAMS) will become the first formed WD and the more massive WD at the time of the merger, though this is not always the case for all evolutionary channels. However, throughout the paper, we define the primary (with mass  $m_p$ ) as the star which ends up as the more massive WD at the time of the merger, and the companion is the secondary (with mass  $m_s$ ). We illustrate the onset of the most important evolutionary stages in Fig. 2 with Roman numerals (I–X), where time  $t$ , masses  $m_p$  and  $m_s$ , and separation  $a$  are indicated in Myr,  $M_{\odot}$  and  $R_{\odot}$ , respectively. We also show the mass evolution of the binary in Fig. 3.

Our example begins with two MS stars on a circular orbit with an orbital period of 8.3 h ( $a=37 R_{\odot}$ , **stage I**). On the ZAMS,  $m_p$  and  $m_s$  are  $5.65$  and  $4.32 M_{\odot}$ , and their corresponding radii are  $2.84$  and  $2.43 R_{\odot}$ , respectively. At 79 Myr the primary evolves off the MS and fills its Roche-lobe, leading to RLOF while in the Hertzsprung Gap (**stage II**).<sup>2</sup> The mass ratio is fairly close to unity, so RLOF is stable ( $f_a = 0.5$ ) though it initially proceeds on a thermal time-scale. Over the course of RLOF, which lasts 0.15 Myr, there is a mass ratio reversal, where the primary becomes the less massive star. The mass transfer (from less massive to more massive star) and expansion of the primary drive an increase in separation to  $233 R_{\odot}$ , the primary shrinks back inside its Roche-lobe and RLOF ceases. By the time RLOF has stopped,  $m_p = 1.02 M_{\odot}$  while  $m_s$  has increased to  $6.62 M_{\odot}$ . The primary continues to evolve up the red giant branch, though by this point most of its hydrogen-rich layers have been removed in RLOF. Once the hydrogen shell-burning phase is complete, the primary becomes a naked helium star (core of red giant). At  $t=99$  Myr, the primary becomes a slightly evolved naked helium star and increases significantly in size. At  $t=102$  Myr, the primary fills its Roche-lobe and a second phase of stable RLOF ensues (**stage III**). Helium-rich material is transferred to the secondary on a nuclear time-scale for 0.14 Myr (as before  $f_a = 0.5$ ). Mass transfer ceases at a separation of  $a = 318 R_{\odot}$ , when  $m_p = 0.86 M_{\odot}$  and  $m_s = 6.67 M_{\odot}$ . By this stage in the evolution, the primary has converted much of its helium core into CO, and upon completion of helium burning at  $t = 102$  Myr, it becomes a CO WD (**stage IV**).

At  $t=115$  Myr, the primary begins its journey up the red giant branch. Once the secondary reaches a radius of  $123 R_{\odot}$  (orbital period of 140 d), a CE takes place (**stages V, VI**), leaving behind the CO WD and the (naked) core of the red giant, a decreased separation (orbital period of 261 min) and  $m_s = 1.27 M_{\odot}$  (**stage VII**). At  $t = 127$  Myr, the secondary becomes a slightly evolved naked helium star. Soon afterwards it fills its Roche-lobe which leads to a third RLOF phase (**stage VIII**).

<sup>2</sup> See Belczynski et al. (2008, sect. 5.6) for a description of how stellar rejuvenation is treated in STARTRACK.

The mass transfer rate initially proceeds on a thermal time-scale and is fairly high ( $\dot{M}_{\text{tran}} = 8.8 \times 10^{-5} M_{\odot} \text{ yr}^{-1}$ ). For the given WD accretor mass, such a mass transfer rate is above the critical threshold that leads to 100% burning efficiency (the critical value is  $4.57 \times 10^{-7} M_{\odot} \text{ yr}^{-1}$  for  $0.84 M_{\odot}$  WD, interpolated from Kato & Hachisu 2004, Equation 6). However, the mass transfer rate is super-Eddington, and so the accretion rate is capped at the Eddington accretion rate ( $\dot{M}_{\text{accr}} = 2.0 \times 10^{-5} M_{\odot} \text{ yr}^{-1}$ ; Eddington accretion lasting 0.002 Myr).<sup>3</sup> The mass transfer rate soon after enters the nuclear time-scale regime, and as it decreases helium burning continues to be stable on the CO WD. Once the mass transfer rate drops below  $\dot{M}_{\text{tran}} = 1.74 \times 10^{-6} M_{\odot} \text{ yr}^{-1}$  (still  $t = 128$  Myr; WD mass  $1.08 M_{\odot}$ ), helium burning is no longer stable (Equation 4, Kato & Hachisu 2004) and thus not fully efficient. The primary continues to accrete another  $0.11 M_{\odot}$  (total mass transfer including Eddington-limited phase lasts 0.15 Myr), though RLOF shuts off when the orbit has expanded to  $a = 1.91 R_{\odot}$  (orbital period of 5.2 hr). At this point,  $m_p = 1.19 M_{\odot}$  and  $m_s = 0.78 M_{\odot}$ , while the secondary’s helium core is almost completely burned to CO ( $m_{\text{core}} = 0.76 M_{\odot}$ ). Within  $10^5$  yr (after losing  $\sim 0.001 M_{\odot}$  in stellar winds) the secondary becomes a CO WD (stage IX). The two WDs evolve toward smaller orbital separations over the next Gyr under the influence of gravitational wave radiation, and merge at  $t = 1259$  Myr (stage X), with a combined mass of  $1.96 M_{\odot}$ . Such a delay time (1259 Myr) is typical of double degenerate mergers – they are predicted to produce more SNe Ia at early times, peaking at a few hundred Myr though still producing a significant number of events  $\gtrsim 1 - 3$  Gyr (e.g. fig. 1, Ruiter et al. 2009).

The system described above is typical of an evolutionary channel in which the critical accretion phase onto a WD (hereafter stage VIII, cf. Fig. 2) occurs. For the evolutionary model under consideration ( $\alpha_{\text{CE}} \lambda = 1$  of Ruiter et al. 2011), we find that 43% of all CO+CO WD merger progenitors undergo such an accretion phase during which the primary WD (e.g. the first-formed and *more massive* WD) accretes an additional  $0.001 - 0.45 M_{\odot}$  after its formation (in the majority of cases it gains  $\sim 0.2 \pm 0.1 M_{\odot}$ ). In addition to these 43%, 9% of merger progenitors encounter the opposite situation: the secondary WD (e.g. the first-formed but *less-massive* WD) undergoes helium accretion.<sup>4</sup> The remaining 48% of progenitors do not encounter a stable mass accretion phase while one of the stars is a WD.

Different physical properties of a binary at birth (masses, mass ratio and separation/eccentricity) influence the ensuing evolution. We find that for the (43%) group of primary interest, typical ZAMS masses are somewhat large, peaking at  $\sim 4 - 5 M_{\odot}$  (though the entire range is  $2 - 7 M_{\odot}$ ), and initial mass ratios  $q_0$  (= more massive star / less massive star) range  $\sim 1 - 2$  with a peak at  $\sim 1$ . For cases where the WD-accretion phase occurs on the secondary WD (9%), ZAMS masses are in the range  $\sim 2 - 3.5 M_{\odot}$  and thus result in lower-mass WDs (in addition,  $q_0$  for these systems peaks at  $\sim 1.4$ ). For merger progenitors which do not undergo the WD-accretion phase (48%), ZAMS masses are mostly  $\sim 2 - 3 M_{\odot}$ , and

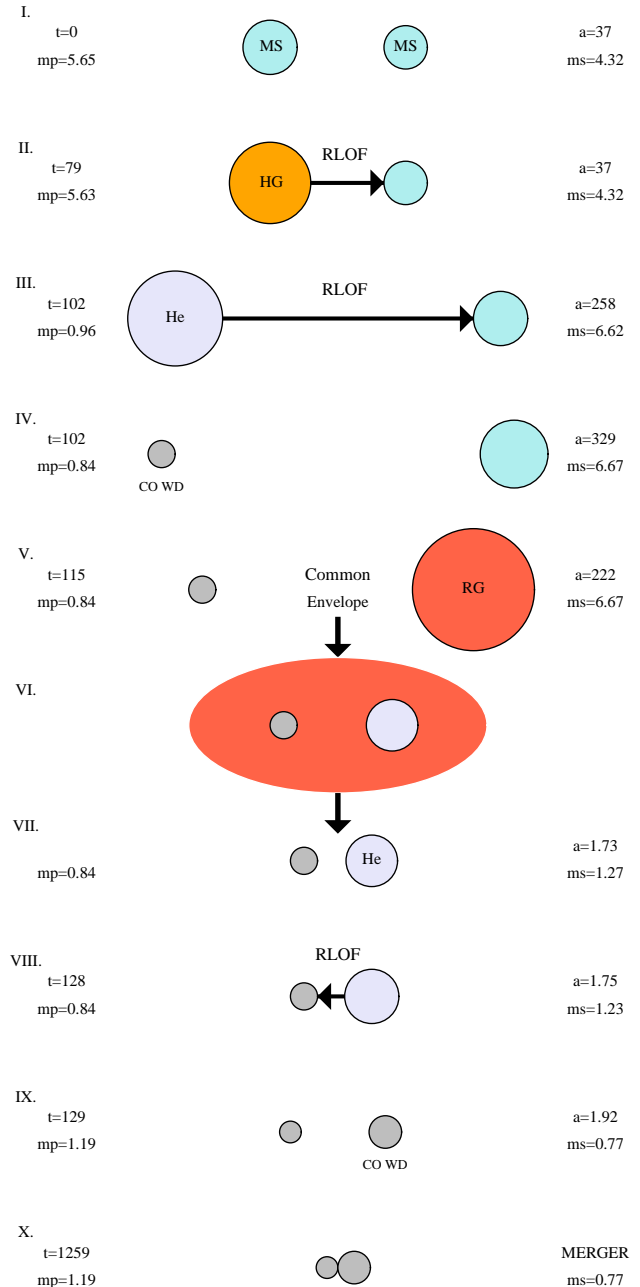


**Figure 2.** Flowchart showing a typical evolutionary channel where the primary WD gains mass via RLOF from its helium star companion, prior to the double CO WD merger. The duration of the RLOF phases and other evolutionary details are given in the text.

<sup>3</sup> If such binaries lead to SNe Ia, we estimate  $\sim$ few to 10 systems to be in this high-accretion phase and thus bright and potentially visible in the Galaxy (Galactic SN Ia rate of  $0.007 \text{ yr}^{-1}$ , Badenes & Maoz 2012, section 4). This number is within observational constraints, and in fact our example system exhibits physical properties similar to those of the helium nova V445 Puppis (Kato et al. 2008).

<sup>4</sup> These secondaries only gain a small amount of mass and they never become the more massive (exploding) WD.

$q_0$  strongly peaks at unity. Hence, a large fraction of these stars evolve at roughly equal rates and in many cases, they reach the short-lived helium star phase at roughly equal times, so stage VIII does not occur.



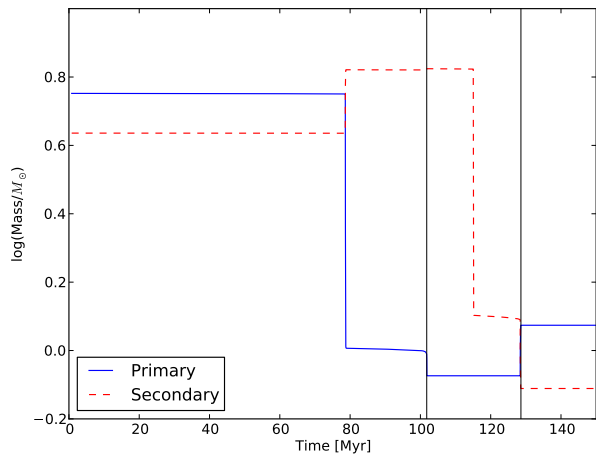


**Figure 3.** Mass evolution for the binary system shown in Fig. 2. We do not show the last  $\sim$ Gyr of evolution since the WD masses remain unchanged during that time. The common envelope event is marked by the drastic decrease in secondary mass at 115 Myr, while the two vertical lines indicate the formation times of the CO WDs.

### 3 CONDITION FOR PROMPT DETONATION

Binary population synthesis calculations provide a predicted distribution of physical parameters for merging CO WD pairs. However, the prompt detonation explosion mechanism of Pakmor et al. (2010, 2011, 2012) is not expected to be realised for all CO WD mergers. As discussed by Pakmor et al. (2010, 2011), conditions favouring a prompt detonation are most plausible when the ratio of the secondary WD mass ( $m_s$ ) to the primary WD mass ( $m_p$ ) is high (approaching 1). In a study of mergers with  $m_p = 0.9 M_\odot$ , Pakmor et al. (2011) determined that the critical mass ratio ( $q_c = m_s/m_p$ ) above which explosion is plausible is  $q_c \sim 0.8$ . The critical  $q$ -value, however, may depend on the mass of the primary, likely having a value that decreases with increasing  $m_p$  (for higher-mass primaries, the densities are higher and the merger is more violent making it easier to reach the conditions needed for triggering a detonation, Seitenzahl et al. 2009). Presently, sufficiently detailed simulations to determine how  $q_c$  will depend on primary mass have not been carried out. Therefore, in this study, we will adopt a simple parametrization of  $q_c$ :

$$q_c = \min\left(0.8 \left(\frac{m_p}{0.9 M_\odot}\right)^{-\eta}, 1.0\right) \quad (1)$$

where  $\eta$  is a parameter that we will use to explore how  $q_c$  influences our findings.

### 4 PRIMARY MASS/PEAK BRIGHTNESS RELATION

Ideally, synthetic observables for a suite of three-dimensional WD merger models would be used to determine the relationship between the system parameters and the explosion brightness. Unfortunately, such simulations are too computationally expensive for this to be practical in this study. However, as argued in Section 1, the peak brightness of a prompt detonation merger model is directly related to the mass of the more massive WD ( $m_p$ ); in the merger, the  $^{56}\text{Ni}$  is mostly synthesized in the detonation of the primary. We

**Table 1.** The peak bolometric magnitude derived from our 1D sub-Chandrasekhar mass pure detonation models for CO WDs for a range of WD masses ( $m_{\text{WD}}$ ).

$m_{\text{WD}} [M_\odot]$	$M_{\text{bol}} [\text{mag}]$
0.81	-13.75
0.88	-16.74
0.97	-18.20
1.06	-18.85
1.10	-19.03
1.15	-19.22
1.28	-19.49

therefore estimate the brightness of a merger from a simple one-dimensional model for a detonation of a WD with mass equal to that of the primary.

To quantify the relationship between the primary mass and the peak bolometric magnitude ( $M_{\text{bol}}$ ), we carried out a series of simulations for detonations of single CO WDs with a range of WD masses ( $m_{\text{WD}} = m_p$ ). These simulations were computed in exactly the same manner as those described by Sim et al. (2010). We constructed hydrostatic models for CO WDs and simulated detonations of these WDs using our SN Ia explosion code. In all cases, the detonations were centrally ignited and their propagation followed using the level-set technique (Golombek & Niemeyer 2005; Fink et al. 2010). Nucleosynthesis in the explosions was computed in a post-processing step using our standard tracer particle approach (Travaglio et al. 2004; Seitenzahl et al. 2010) assuming an initial  $^{12}\text{C}/^{16}\text{O}/^{22}\text{Ne}$  composition of 47.5/50/2.5 % by mass (roughly appropriate for solar metallicity). For each explosion model we performed radiative transfer simulations with ARTIS (Sim 2007; Kromer & Sim 2009) to predict synthetic light-curves (adopting the cd23\_gf-5 atomic dataset of Kromer & Sim 2009).

Our chosen values of  $m_{\text{WD}}$  and the derived values of  $M_{\text{bol}}$  are given in Table 1. Fig. 4 shows the  $m_{\text{WD}}-M_{\text{bol}}$  relationship derived from the models. As expected, the models define a smooth, monotonic relationship between brightness and mass (see e.g. Sim et al. 2010). For the analysis below, we have made a polynomial interpolation between the data points defined by the models to obtain a simple functional form for the  $m_{\text{WD}}-M_{\text{bol}}$  relationship. This interpolated relationship is also shown in Fig. 4. (see Appendix B for coefficients of the fit).

Recently, Pakmor et al. (2012) presented results from a complete simulation of a prompt-detonation model for the merger of a CO WD pair with  $m_p = 1.1$  and  $m_s = 0.9 M_\odot$ . The angle-averaged peak brightness for this model is indicated in Fig. 4. As expected, its peak brightness is very close ( $\Delta M_{\text{bol}} \sim 0.2$  mag) to that of our equivalent single WD detonation model. We also show the angle-averaged peak  $M_{\text{bol}}$  for the complete merger simulation of Pakmor et al. (2010). Again, the agreement with our relation is good, although the difference is slightly larger ( $\Delta M_{\text{bol}} \sim 0.4$  mag). These comparisons lend credence to the approach we adopt to estimate the peak brightness of WD merger models and suggest that our method is accurate to a level of several tenths of a magnitude.

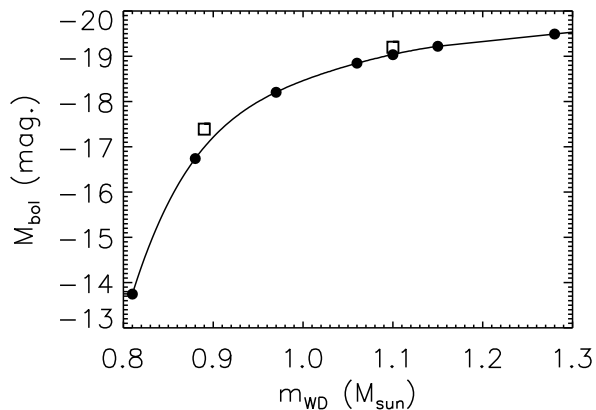


**Figure 4.** The  $m_{\text{WD}}-M_{\text{bol}}$  relationship derived from the pure detonation models in Table 1. The filled circles indicate the data derived from the models and the solid line shows the polynomial interpolation we adopt in our analysis. The squares indicate the results from the full merger simulations described by Pakmor et al. (2010; subluminal) and Pakmor et al. (2012;  $M_{\text{bol}} \sim -19$ ).

## 5 RESULTS

### 5.1 Distribution of brightness

To convert the population synthesis data to a distribution of peak brightness, we first select all systems from the binary population synthesis calculation that lead to CO+CO mergers. From these we identify those systems that will explode based on our mass ratio cut ( $q > q_c$ , and chosen values of  $\eta$ ; Section 3). Finally, we apply our  $m_{\text{WD}}-M_{\text{bol}}$  relationship (Section 4) to derive the peak brightness for each system from its primary WD mass. We exclude from our analysis systems in which the primary WD is  $m_p < 0.8 M_\odot$ , for two reasons. First, for such small primary masses the low densities make it extremely challenging to ignite the detonation. Second, at low mass the  $^{56}\text{Ni}$  yield is expected to be too small to give rise to a bright transient even if a prompt detonation were to occur (see Table 1). This effectively removes the majority of systems associated with the low- $m_{\text{WD}}$  peak ( $\sim 0.65 M_\odot$ ) from our analysis: those systems are not promising candidates for the prompt detonation scenario (although it has been suggested that explosion of such systems might still occur, van Kerkwijk et al. 2010; but see also Shen et al. 2012).

Our computed brightness distribution is plotted in Fig. 5 for three representative values of the  $\eta$ -parameter in our prescription for  $q_c$  (see Equation 1). We have restricted  $\eta$  to be positive, ensuring that the critical  $q$ -value decreases with increasing  $m_p$  (except for the case where  $\eta = 0$ , where  $q_c = 0.8$  for all values of  $m_p$ ). We find that for  $\eta \geq 1.5$ , nearly all of the primaries at the high-mass end are included, so adopting larger values of  $\eta$  is unnecessary. Thus, we choose two values of  $\eta$  which bracket the physically-realistic extremes:  $\eta = 0$  and  $\eta = 1.5$ , and a third value  $\eta = 0.75$  (the mid-

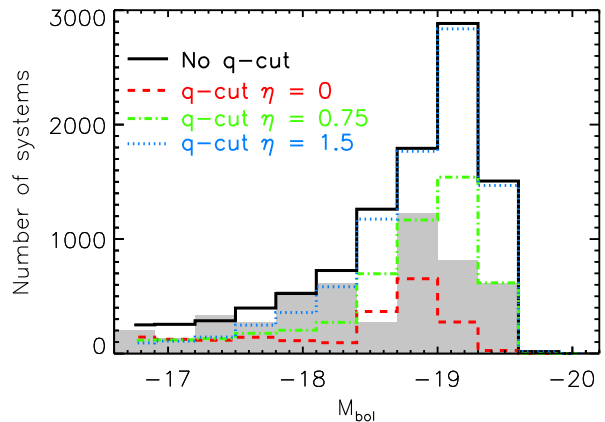


**Figure 5.** The predicted distribution of peak bolometric magnitude ( $M_{\text{bol}}$ ) obtained by combining the primary WD masses from the model of Ruiter et al. (2011) with our  $m_{\text{WD}}-M_{\text{bol}}$  relationship (Fig. 4). The black line shows the results assuming that all mergers successfully lead to a prompt detonation. The coloured lines show the effect of imposing cuts on the  $q$ -value of the merger (requiring that  $q > q_c$ ) for different values of  $\eta$  (see text). The grey histogram shows the absolute magnitude distribution derived from a volume-limited sample of SNe Ia by Li et al. (2011, see their fig. 5). To facilitate comparison of the shapes, the observational data have been scaled to match the number of systems in our calculation for  $\eta = 0.75$ .

point), simply for illustrative purposes.<sup>5</sup> We also show the result without any  $q$ -cuts (i.e. all population synthesis data).

As shown in Fig. 5, our  $m_{\text{WD}}-M_{\text{bol}}$  relationship converts the higher mass peak of the  $m_p$  distribution (Fig. 1, solid line) into a brightness distribution with a clear peak around  $M_{\text{bol}} \simeq -19$  mag, a short tail of brighter events, and a long tail stretching to fainter magnitudes. The amplitude of the peak and to some degree its location depend on our choice of  $\eta$ . For  $\eta = 1.5$  (or higher), the high  $M_{\text{bol}}$  part of the distribution is almost insensitive to the choice of  $\eta$  but for smaller values (e.g.  $\eta = 0$ ), a significant fraction of the high  $m_p$  systems are excluded. However,  $\eta$  does not qualitatively affect our findings: the peak around  $M_{\text{bol}} \sim -19$  mag is present in all cases – it is a consequence of the underlying shape of the  $m_p$  distribution in merging systems and the steepness of our  $m_{\text{WD}}-M_{\text{bol}}$  relationship.

### 5.2 Comparison to observations

Recently, Li et al. (2011) presented pseudo-observed luminosity functions for SNe Ia based on a sample of objects within 80 Mpc from the Lick Observatory Supernova Search (LOSS, see e.g. Leaman et al. 2011, for details). We compare the shape of their volume-limited luminosity function to the results of our calculations in Fig. 5. In this comparison, we include all 74 of their SNe Ia (regardless of sub-type and host galaxy type) and, for convenience, have arbitrarily rescaled the distribution to match the total number of SNe Ia to that of our calculation for  $\eta = 0.75$ .

<sup>5</sup> We note that for our evolutionary example of a violent merger formation channel described in Section 2.3 ( $q_{\text{merger}} = m_s/m_p = 0.774/1.185 = 0.653$ ), the necessary criteria leading to a SN Ia are satisfied for  $\eta > 0.74$ :  $\eta = 1.5 \rightarrow q_c = 0.530$ ;  $\eta = 0.75 \rightarrow q_c = 0.651$ .

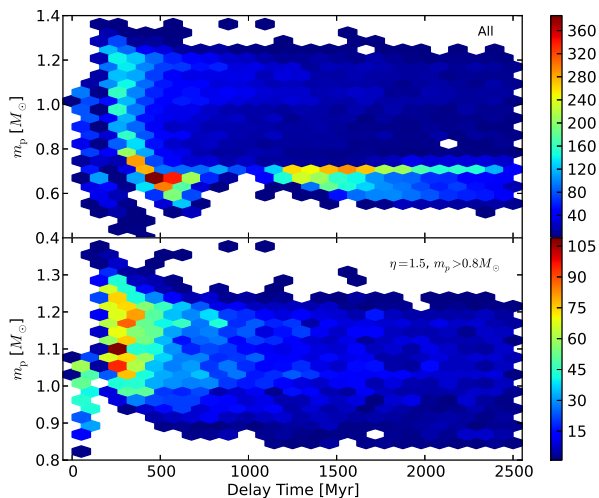


**Figure 6.** Primary WD mass ( $m_p$ ) vs. delay time up to 2500 Myr for STARTRACK CO+CO WD mergers. The upper panel shows all systems while the lower panel only includes systems that pass the  $q_c$  criterion with  $\eta = 1.5$  and  $m_p > 0.8M_\odot$ . Note the different scaling for the two plots. It is evident that the most massive primaries preferentially merge at prompt delay times: for both panels  $\gtrsim 95\%$  of systems with  $m_p > 1.3M_\odot$  have delay times  $< 1$  Gyr. Mergers with  $m_p > 1.3M_\odot$  make up 0.2% of all CO+CO mergers and 0.5% of  $\eta = 1.5$ ,  $m_p > 0.8M_\odot$  mergers. We also note that the first progenitors to explode are not from binaries with the most massive primaries (see text for details).

This comparison suggests that the prompt detonation violent merger scenario could give rise to a brightness distribution of SNe Ia that is fairly compatible with observations. In particular, the standard model of Ruiter et al. (2011) predicts a large fraction of explosions within a fairly narrow range of peak magnitude ( $\Delta M_{\text{bol}} \sim 1$  mag) centred around  $M_{\text{bol}} \sim -19$  mag, as is observed.

There are a number of important caveats to consider when interpreting the comparison in Fig. 5. First, the supernovae in the Li et al. (2011) luminosity function have been corrected for Galactic extinction but not for host galaxy reddening, thus variations in extinction from object to object will be responsible for some component of the tail to lower peak magnitudes in the observed sample. Second, the Li et al. (2011) data are not derived from complete sets of colour light-curves but are available only for the  $R$ -band. However, this is not expected to significantly affect our results around the peak of our distribution: in the complete merger simulation presented by Pakmor et al. (2012), the difference in peak bolometric and  $R$ -band magnitudes was  $M_{\text{bol}} - M_R = 0$ . We note that  $M_{\text{bol}} - M_R$  is expected to become positive for sub-luminous mergers but for the systems of interest, this should not be large effect compared to the bin size in Fig. 5 (in the simulation of Pakmor et al. 2010,  $M_{\text{bol}} - M_R \sim 0.4$  mag.). Third, our analysis neglects any influence of observer orientation on the explosion brightness – the Pakmor et al. (2010, 2012) simulations suggest that orientation may cause variations of around  $\pm 0.4$  mag. Nevertheless, although quantitatively important, none of the effects is expected to qualitatively change our result.

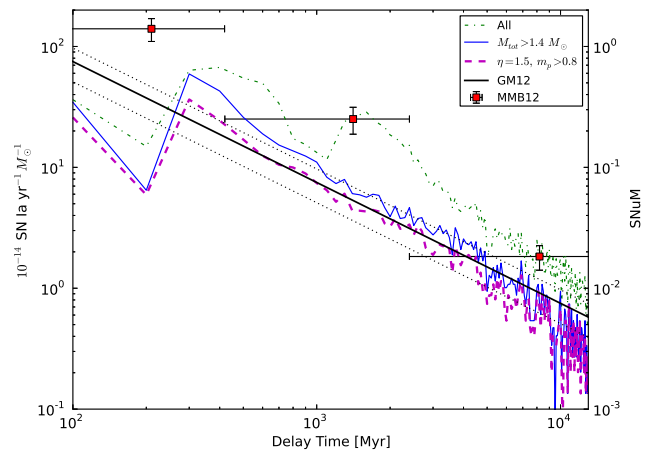


**Figure 7.** STARTRACK smoothed DTD of all CO+CO mergers (green dots), CO+CO mergers where  $M_{\text{tot}} > 1.4M_\odot$  (blue solid), and CO+CO WD mergers which satisfy our criteria  $\eta = 1.5$  and  $m_p > 0.8M_\odot$  (magenta dashes). The small fluctuations are due to Monte Carlo noise. Over-plotted with red squares is the best-fit DTD derived from SDSS data, the three time bins are indicated by horizontal error bars:  $t < 0.42$  Gyr,  $0.42 < t < 2.4$  Gyr and  $t > 2.4$  Gyr (see Maoz et al. 2012, MMB12). The smooth black solid line shows the best-fit DTD from Graur & Maoz (2012, GM12), with systematic uncertainties (thinner dotted lines). The right-axis shows units in SNuM: number of SN Ia per  $10^{10}M_\odot$  formed in stars per century.

### 5.2.1 Brightness and delay time

We note the important finding that, while fairly massive WDs with masses of  $\sim 1.2M_\odot$  may explode at any delay time  $> 150$  Myr, the most massive ones ( $\geq 1.3M_\odot$ ) only explode as prompt events, with rare exceptions (see Figure 6). This finding supports the observational evidence for more luminous SNe Ia occurring among younger stellar populations (Brandt et al. 2010). At the same time however, the events with the shortest delay times ( $< 100$  Myr) are not from the most massive primaries: these occur via rarer formation channels where (usually) the secondary initiates two CE events. These ‘ultra-prompt’ double CE systems do not undergo phase VIII mass accretion, though they are still massive enough to be considered SNe Ia progenitors in our model. The difference in evolutionary timescale between these double CE events and all of the other formation channels is the cause of the dearth of mergers at  $\sim 150$  Myr in Figure 6. For the majority of the events at later delay times only one CE is encountered, as is expected (Ruiter et al. 2009; Mennekens et al. 2010).

### 5.2.2 Rates and DTD

We have not attempted to calibrate the population synthesis event frequency of CO+CO violent mergers to compare directly with the SN Ia rates of Li et al. (2011). To do so would require us to adopt a model for the star-formation history associated with their volume-limited sample, which would introduce unwanted uncertainties. Nonetheless, we can compare our theoretical DTD to that from observations. Merging CO+CO WD pairs are currently the favoured theoretical scenario for producing a relatively high number of SN Ia progenitors compared to other long-standing progenitor models (Iben & Tutukov 1984; Yungelson et al. 1994; Ruiter et al. 2009). In Figure 7 we show three theoretical DTDs for WD mergers as-

suming a binary fraction<sup>6</sup> of 70%: All CO+CO WDs, mergers for which  $M_{\text{tot}} > 1.4 M_{\odot}$  (DDS), and systems which meet our criteria  $\eta = 1.5$  and  $m_p > 0.8 M_{\odot}$  (violent mergers). Additionally we show two of the most up-to-date observationally-recovered DTDs from the literature: Maoz et al. (2012, SDSS II galaxies; fig. 1) and Graur & Maoz (2012, field rates; fig. 12).

The DTD from violent mergers (magenta dashed line) compares rather well with the most recent observational DTD estimates. At long delay times ( $t > 2.4$  Gyr) the violent merger DTD falls within the observational uncertainties of Maoz et al. (2012). Also, the model agrees very well with the best-fit DTD from Graur & Maoz (2012) for delay times above 300 Myr, implying that violent mergers might be a dominant contributor to SNe Ia in field galaxies (see Graur & Maoz 2012, for a comparison of observational DTDs from recent works).

Up until now, there has been a notable discrepancy between observed rates of SNe Ia – in particular at early delay times – and the rates calculated from population synthesis. Typically, binary population synthesis rates (as a function of delay time) were too low to explain the observed numbers. This discrepancy remains an open issue, though some possible reasons have been discussed<sup>7</sup> (see Nelemans et al. 2012; Ruiter et al. 2011, sect. 4.1; see also Mennekens 2010 who point out that rotation may increase the likelihood for explosion in WD mergers). However, the new observationally-derived DTD of Graur & Maoz (2012) has a lower amplitude (implying lower SN Ia rates) than those from previous observations. This brings our theoretical DTD, as well as some theoretical DTDs from other groups, into better agreement with observations. It should be noted that Graur & Maoz (2012, sect. 6) mention that their best-fit power-law DTD might be underestimated, since it was derived using predominantly old galaxies.

## 6 DISCUSSION

We have found that, in the standard model of Ruiter et al. (2011), a certain formation channel is critical for creating massive primary WDs. In Section 2.3 we described the typical evolution of a binary which produces two merging CO WDs where the primary WD is particularly massive due to an important evolutionary phase: it accretes (in that case  $0.35 M_{\odot}$ ) from a helium-rich companion star. Within the model framework of Ruiter et al. (2011), such a phase of RLOF occurs for a significant fraction (43%) of the CO+CO WD merger progenitors.

We have mapped the (exploding) primary WD masses for all CO+CO WD mergers on to magnitude-space using our  $m_{\text{WD}}-M_{\text{bol}}$  relation, and have presented the results for a series of  $q$ -cuts (Fig. 5). Regardless of the  $q$ -cut used, the shape of our theoretical  $M_{\text{bol}}$  distribution for merging primary WDs is quite striking, since it matches well with the observed  $M_{\text{bol}}$  distribution for SNe Ia of Li et al. (2011). *Our results indicate that double degenerate mergers exploding in the violent merger scenario show exceptional promise as progenitors of SNe Ia.*

However, despite these very encouraging results, we point out in the next two sub-sections some important issues to keep in mind,

which could have a significant effect on the evolutionary outcomes for close binaries, in turn affecting the impact of these new findings.

### 6.1 A key assumption: Common Envelope parametrization

Different assumed CE parametrizations have a critical impact on which evolutionary channels lead to the formation of close binaries, as well as how often they form and how often they merge (Dominik et al. 2012). So, we now discuss how the results found above are sensitive to the choice of the adopted CE formalism and CE efficiency.

Considering a lower CE efficiency such as  $\alpha_{\text{CE}} = 0.5$  with  $\lambda = 1 \rightarrow \alpha_{\text{CE}}\lambda = 0.5$ , which is often used in population synthesis, we find that the stage VIII accretion phase is indeed encountered though not as often as in the standard model (33% vs. 43%). Quantitatively speaking, the overall merger rates from population synthesis calculations for this CE model are about a factor of two lower than the standard model (Ruiter et al. 2009), since a larger number of progenitors which make CO+CO WD mergers in the standard model will merge before a double WD is formed in a lower CE efficiency model. Qualitatively however, there is little difference between the two models, and in the  $\alpha_{\text{CE}}\lambda = 0.5$  model we still expect such a ‘stage VIII’ accretion phase to occur leading (favourably) to more massive primary WDs.

For the case of very low CE efficiency, such as that investigated in Ruiter et al. (2011) ( $\alpha_{\text{CE}} = 0.25$  with  $\lambda = 0.5 \rightarrow \alpha_{\text{CE}}\lambda = 0.125$ ), stage VIII is almost never encountered: less than 1% of binaries go through this evolutionary channel (> 99% of primary WDs do not experience accretion before the merger). In that calculation, the formation channels that do lead to CO+CO WD mergers are altogether different from our standard case. For the  $\alpha_{\text{CE}}\lambda = 0.125$  model, binaries which end up merging as CO+CO WDs generally start out with larger semi-lata recta ( $a \times (1.0 - e^2)$ ) of  $\sim 50 - 250 R_{\odot}$ , while for the standard model initial semi-lata recta typically range from  $20 - 100 R_{\odot}$ . For these merging WD pairs, the primary WDs are in general less massive than their standard model counterparts.

The 0.2% of CO+CO WD merger progenitors which do encounter the stage VIII accretion phase in the  $\alpha_{\text{CE}}\lambda = 0.125$  model are born with near-equal masses, are closer at birth (semi-lata recta  $20 - 100 R_{\odot}$ ), and the first-formed WD always forms either during or after the CE (in contrast to our standard example, where it forms prior to the CE event). In all of these systems, there is a mass ratio reversal during the evolution, which is significant enough to allow for rapid rejuvenation of the secondary and the secondary is the first star to evolve into a WD (this process is also encountered on occasion in the standard model; Section 2.3). However, these binaries do not meet our criteria for SN Ia progenitors: the most massive primary WD (at merger) in the 0.2% group is  $0.7 M_{\odot}$ . This stems from the fact that the ZAMS progenitor masses for this channel are quite low ( $\sim 1.9 M_{\odot}$ ). In any case, as demonstrated in Ruiter et al. (2011) the expected rate of merging CO+CO WDs is extremely low for this CE model.

If we consider the ‘ $\gamma$ -formalism’ for CE evolution (e.g. Nelemans et al. 2000), which was assumed for all CE events for model G1.5 in Ruiter et al. (2011), stage VIII is also not encountered very often. The typical formation channels which lead to double WDs from the standard model do not make double WDs in the ‘ $\gamma$ -formalism’ model, since for the latter the stars have larger orbits post-CE, and will not merge within a Hubble time. Four % of primary CO WDs undergo stage VIII mass accretion, while for 3% it is the secondary WD for which the phase occurs. Both groups

<sup>6</sup> For stars of spectral type B3-B7, which are typical progenitors of violent WD mergers, the binary fraction is estimated to lie between 40-100 % (Hoffmeister et al. 2011). We do not consider higher multiplicity here.

<sup>7</sup> Observational samples which include massive elliptical galaxies tend to exhibit DTDs which have higher SN rates than volume-limited samples, D. Maoz, private communication 2012; see also Maoz et al. (2012).



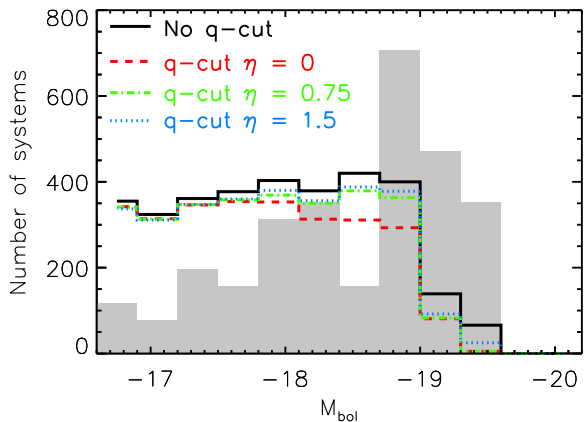


**Figure 8.** As Fig. 5 but using the WD masses as they were *at birth*. No matter which  $q$ -cut is used, no theoretical  $M_{\text{bol}}$  distributions exhibit a shape similar to the absolute magnitude distribution of SNe Ia from Li et al. (2011).

have  $q_0 = \gtrsim 1.2$ , and often the first interacting event is a CE, followed by a second CE after the primary has evolved into a CO WD. Both CE events enable the stars to be on a close enough orbit such that RLOF between a slightly evolved helium star and the primary WD is possible. In terms of frequency of events, the corresponding DDS model of Ruiters et al. (2011) yields a rate which is 10% of that of the standard model, thus we would expect a smaller fraction of potential SN Ia progenitors from violent mergers to be produced via the G1.5 model.

Not surprisingly, binary population synthesis predictions for double degenerate mergers are rather sensitive to the assumed CE parametrization. In summary, a small reduction of CE efficiency ( $\alpha_{\text{CE}}\lambda = 1 \rightarrow 0.5$ ) does not qualitatively affect our results. However a very low efficiency ( $\alpha_{\text{CE}}\lambda = 0.125$ ) or use of the  $\gamma$ -prescription alone dramatically reduces both the total merger rate and the fraction of systems that undergo the stage VIII accretion phase. We note additionally that using a higher CE-ejection efficiency ( $\alpha_{\text{CE}} > 1$ , Meng & Yang 2012) should lead to a larger number of WD mergers.

## 6.2 WD mass growth: implications

As an experiment to confirm that the mass-growth of the primary WD after it is born is key to our findings, in Fig. 8 we show results equivalent to Figure 5 but using the STARTRACK WD primary masses *at their birth* (dashed line in Figure 1) rather than at explosion. It is immediately obvious that the shape of the observed absolute magnitude distribution of Li et al. (2011) is not reproduced in this case. Rather, for all  $q$ -cuts used, the theoretical  $M_{\text{bol}}$  distribution is rather flat from  $-17$  to  $-19$  mag, with a steep drop-off at  $M_{\text{bol}} = -19$  mag.

While Fig. 8 is only an experiment and not a self-consistent calculation for our STARTRACK simulations, it may be roughly representative of predictions from alternative models. In particular, we note that other population synthesis codes predict a *total* CO+CO WD merger mass distribution that is fairly smooth (Nele-

mans 2010<sup>8</sup>; see also Bogomazov & Tutukov 2010, fig. 1), in contrast to the total mass distribution from STARTRACK which has a second peak as a consequence of stage VIII (cf. Fryer et al. 2010 fig. 3). We have identified an evolutionary channel that produces fairly massive primary WDs via helium-accretion, though it remains to be established whether such a prediction is confirmed by future observations (see Footnote 3). In addition, improved input physics from models of interacting binaries that incorporate detailed stellar structure – in particular for helium star models – are needed to properly address the issue of mass transfer/accretion in close binaries (see e.g. Eggleton et al. 2011).

## 6.3 Ultra-prompt mergers

As mentioned in section 5.2.1, the SNe Ia from WD mergers with delay times  $< 100$  Myr (‘ultra-prompt’) are formed by way of a double CE: the initially less massive star loses its H-rich envelope while in the Hertzsprung gap or on the giant branch, and then later loses its He-rich envelope when it is a somewhat-evolved helium star. We find that 0.5% of all CO+CO mergers which have primary WD masses  $> 0.9M_{\odot}$  merge less than 1000 yr after the last CE. The fraction is raised to 4% if the merger occurs within 10,000 yr after the last CE. This has very interesting implications for at least a couple of reasons. The post-explosion spectra of these mergers are likely to show signatures of circumstellar material – thus far thought to be a likely signature of a single degenerate scenario SN Ia (Sternberg et al. 2011). On the other hand, since the primary WD will still be quite hot upon merging, these binaries may meet the necessary criteria for producing ‘core degenerate’ mergers (see Ilkov & Soker 2012), which might produce SNe Ia – or some other bright transient – at a delay time larger than the merger time shown in Fig. 7. In any case, these types of mergers might contribute a small fraction to the population of sub-luminous SNe Ia.

## 6.4 Violent vs. non-violent mergers

Chen et al. (2012) used population synthesis to calculate rates of SNe Ia from CO+CO WD mergers and imposed some additional constraints, namely that in a dynamical merger some fraction of the total mass would be lost from the binary, in turn lowering the probability for a thermonuclear explosion. They found a possible upper limit of SNe coming from “violent mergers” to be about a factor of 5 lower than previous estimates from population synthesis. We would like to point out that by our definition, the mergers considered in Chen et al. (2012) are not violent mergers. In the violent mergers of Pakmor et al. (2012) – on which the Chen et al. (2012) dynamically-motivated restrictions are based – no mass is lost in the merger itself. In the violent merger, the mass transfer phase is very short-lived, and the explosion takes place at the time of the merger at which point all of the matter is swept up (Pakmor et al. 2012). By contrast, the mergers assumed to undergo mass-loss considered by Chen et al. (2012) are likely to exhibit properties of non-violent mergers, where a hot envelope is accreted onto the primary WD. In such a case, a non-negligible amount of material might be ejected from the binary (e.g. Fryer et al. 2010, but see also Dan et al. 2012), though as already discussed, it is not clear that such systems will produce SNe Ia.

<sup>8</sup> Workshop on “Observational Signatures of Type Ia Supernova Progenitors”, Leiden 2010 (<http://www.lorentzcenter.nl/lc/web/>).

## 7 SUMMARY

We find that the distribution of merging CO WD pairs predicted by the STARTRACK binary evolution population synthesis code gives rise to a range of explosion brightnesses via the prompt detonation (violent merger) mechanism (Pakmor et al. 2010, 2012) that is compatible with observed SNe Ia (Fig. 5). Further, the DTD (Fig. 7) agrees well with the observed DTD fit from Graur & Maoz (2012), and as shown by Fig. 6 (lower panel), even gives rise to brighter SNe Ia preferentially at short delay times – a trend that is corroborated by SN Ia observations (e.g. Wang & Han 2012).

We have identified that the good agreement with the brightness distribution of Li et al. (2011) depends critically on a particular evolutionary phase during which the first-formed WD accretes mass from a companion which is a slightly evolved naked helium star (stage VIII, Fig. 2). In the standard population synthesis model of Ruiter et al. (2011), nearly half of the CO+CO WD merger progenitors pass through such an accretion phase.

Alternatively, if the critical He-rich accretion phase is not readily realised in nature, then the predicted explosion brightness distribution is not a good match to observations (Fig. 8), likely indicating that a different explosion scenario must dominate and drive the underlying shape of the SN Ia observed brightness distribution. Consequently, our results suggest that detailed studies of helium accretion in binary systems will be a vital step toward establishing the plausibility of the violent merger model for a significant fraction of SNe Ia.

## ACKNOWLEDGMENTS

The authors thank the anonymous referee for comments, as well as Gijs Nelemans for helpful comments on this manuscript. AJR and SAS thank Richard Stancliffe and Brian Schmidt for stimulating discussions. AJR thanks Silvia Toonen, Joke Claeys and Nicki Mennekens for insightful discussions on pertinent topics in binary star evolution and mass transfer, as well as Dan Maoz and Rosanne di Stefano for informative conversation. AJR also thanks Or Graur for kindly sending us data information. RP, MK and ST thank Brian Schmidt for hosting their visit to *The Research School of Astronomy & Astrophysics of the Australian National University*, during which part of this work was carried out. The work of FKR and MF was supported by Deutsche Forschungsgemeinschaft via the Emmy Noether Program (RO 3676/1-1). FKR received funding from the ARCHES prize of the German Federal Ministry of Education and Research (BMBF). IRS was supported by the graduate school “Theoretical Astrophysics and Particle Physics” at the University of Würzburg (GRK 1147). SAS, MK, FKR and MF acknowledge financial support by the Group of Eight/Deutscher Akademischer Austausch Dienst (Go8/DAAD) Australian-German Joint Research Co-operation Scheme (‘Supernova explosions: comparing theory with observations.’). This research was undertaken with the support of resources provided by the Jülich Supercomputing Centre in Jülich, Germany (project HMU14) and the *NCI National Facility* in Canberra, Australia, which is supported by the Australian Commonwealth Government.

## REFERENCES

- Badenes, C., & Maoz, D. 2012, *ApJ Lett.*, 749, L11  
 Barbary, K., Aldering, G., Amanullah, R., et al. 2012, *ApJ*, 745, 32  
 Belczynski, K., Kalogera, V., & Bulik, T. 2002, *ApJ*, 572, 407  
 Belczynski, K., Kalogera, V., Rasio, F. A., et al. 2008, *ApJ Supp.*, 174, 223  
 Benetti, S., Cappellaro, E., Mazzali, P. A., et al. 2005, *ApJ*, 623, 1011  
 Bianco, F. B., Howell, D. A., Sullivan, M., et al. 2011, *ApJ*, 741, 20  
 Blondin, S., Kasen, D., Röpke, F. K., Kirshner, R. P., & Mandel, K. S. 2011, *MNRAS*, 417, 1280  
 Bloom, J. S., Kasen, D., Shen, K. J., et al. 2012, *ApJ Lett.*, 744, L17  
 Bogomazov, A., & Tutukov, A. V. 2010, 25th Texas Symposium on Relativistic Astrophysics  
 Branch, D., Dang, L. C., & Baron, E. 2009, *PASP*, 121, 238  
 Brandt, T. D., Tojeiro, R., Aubourg, É., et al. 2010, *AJ*, 140, 804  
 Chen, X., Jeffery, C. S., Zhang, X., & Han, Z. 2012, *ApJ Lett.*, 755, L9  
 Chomiuk, L., Soderberg, A. M., Moe, M., et al. 2012, *ApJ*, 750, 164  
 Dan, M., Rosswog, S., Guillochon, J., & Ramirez-Ruiz, E. 2012, *MNRAS*, 422, 2417  
 de Kool, M. 1990, *ApJ*, 358, 189  
 Dewi, J. D. M., & Tauris, T. M. 2000, *A&A*, 360, 1043  
 Dominik, M., Belczynski, K., Fryer, C., et al. 2012, *arXiv:1202.4901*  
 Eggleton, P. P., Tout, C., Pols, O., et al. 2011, *Astrophysics Source Code Library*, record ascl:1107.008, 7008  
 Fink, M., Röpke, F. K., Hillebrandt, W., et al. 2010, *A&A*, 514, A53  
 Fryer, C. L., Ruiter, A. J., Belczynski, K., et al. 2010, *ApJ*, 725, 296  
 Ganeshalingam, M., Li, W., & Filippenko, A. V. 2011, *MNRAS*, 416, 2607  
 García-Senz, D., Bravo, E., & Woosley, S. E. 1999, *A&A*, 349, 177  
 Golombek, I., & Niemeyer, J. C. 2005, *A&A*, 438, 611  
 Graur, O., Poznanski, D., Maoz, D., et al. 2011, *MNRAS*, 417, 916  
 Graur, O., & Maoz, D. 2012, *arXiv:1209.0008 (GM12)*  
 Hancock, P. P., Gaensler, B. M., & Murphy, T. 2011, *ApJ Lett.*, 735, L35  
 Hayden, B. T., Garnavich, P. M., Kasen, D., et al. 2010, *ApJ*, 722, 1691  
 Hoffmeister, V. H., Nasser, A., & Chini, R. 2011, *Evolution of Compact Binaries*, 447, 73  
 Horesh, A., Kulkarni, S. R., Fox, D. B., et al. 2012, *ApJ*, 746, 21  
 Hurley, J. R., Pols, O. R., & Tout, C. A. 2000, *MNRAS*, 315, 543  
 Iben, I., Jr., & Tutukov, A. V. 1984, *ApJ Supp.*, 54, 335  
 Iben, I., Jr., & Livio, M. 1993, *PASP*, 105, 1373  
 Ilkov, M., & Soker, N. 2012, *MNRAS*, 419, 1695  
 Ivanova, N. 2011, *ApJ*, 730, 76  
 Ivanova, N., & Chaichenets, S. 2011, *ApJ Lett.*, 731, L36  
 Kasen, D., Röpke, F. K., & Woosley, S. E. 2009, *Nature*, 460, 869  
 Kasen, D. 2010, *ApJ*, 708, 1025  
 Kato, M., & Hachisu, I. 1999, *ApJ Lett.*, 513, L41  
 Kato, M., & Hachisu, I. 2004, *ApJ Lett.*, 613, L129  
 Kato, M., Hachisu, I., Kiyota, S., & Saio, H. 2008, *ApJ*, 684, 1366  
 Kerzendorf, W. E., Schmidt, B. P., Asplund, M., et al. 2009, *ApJ*, 701, 1665  
 Kromer, M., & Sim, S. A. 2009, *MNRAS*, 398, 1809  
 Kromer, M., Fink, M., Stanishev, V., et al. 2012, *arXiv:1210.5243*

Leaman, J., Li, W., Chornock, R., & Filippenko, A. V. 2011, MNRAS, 412, 1419  
 Li, W., Leaman, J., Chornock, R., et al. 2011, MNRAS, 412, 1441  
 Maoz, D., & Badenes, C. 2010, MNRAS, 407, 1314  
 Maoz, D., Sharon, K., & Gal-Yam, A. 2010, ApJ, 722, 1879  
 Maoz, D., Mannucci, F., & Brandt, T. D. 2012, arXiv:1206.0465 (MMB12)  
 Meng, X., & Yang, W. 2012, A&A, 543, A137  
 Mennekens, N., Vanbeveren, D., De Greve, J. P., & De Donder, E. 2010, A&A, 515, A89  
 Nelemans, G., Verbunt, F., Yungelson, L. R., & Portegies Zwart, S. F. 2000, A&A, 360, 1011  
 Nelemans, G., Toonen, S., & Bours, M. 2012, arXiv:1204.2960  
 Nomoto, K., Saio, H., Kato, M., & Hachisu, I. 2007, ApJ, 663, 1269  
 Pakmor, R., Kromer, M., Röpke, F. K., et al. 2010, Nature, 463, 61  
 Pakmor, R., Hachinger, S., Röpke, F. K., & Hillebrandt, W. 2011, A&A, 528, A117  
 Pakmor, R., Kromer, M., Taubenberger, S., et al. 2012, ApJ Lett., 747, L10  
 Patat, F., Chugai, N. N., Podsiadlowski, P., et al. 2011, A&A, 530, A63  
 Prialnik, D., & Kovetz, A. 1995, ApJ, 445, 789  
 Richardson, D., Branch, D., Casebeer, D., et al. 2002, AJ, 123, 745  
 Ricker, P. M., & Taam, R. E. 2012, ApJ, 746, 74  
 Röpke, F. K., Kromer, M., Seitzzahl, I. R., et al. 2012, ApJ Lett., 750, L19  
 Ruiter, A. J., Belczynski, K., & Fryer, C. 2009, ApJ, 699, 2026  
 Ruiter, A. J., Belczynski, K., Sim, S. A., et al. 2011, MNRAS, 417, 408  
 Ruiz-Lapuente, P., Comeron, F., Méndez, J., et al. 2004, Nature, 431, 1069  
 Sand, D. J., Graham, M. L., Bildfell, C., et al. 2012, ApJ, 746, 163  
 Seitzzahl, I. R., Meakin, C. A., Townsley, D. M., Lamb, D. Q., & Truran, J. W. 2009, ApJ, 696, 515  
 Seitzzahl, I. R., Röpke, F. K., Fink, M., & Pakmor, R. 2010, MNRAS, 407, 2297  
 Seitzzahl, I. R., Ciaraldi-Schoolmann, F., Röpke, F. K. 2011, MNRAS, 414, 2709  
 Shen, K. J., Bildsten, L., Kasen, D., & Quataert, E. 2012, ApJ, 748, 35  
 Sim, S. A. 2007, MNRAS, 375, 154  
 Sim, S. A., Röpke, F. K., Hillebrandt, W., et al. 2010, ApJ Lett., 714, L52  
 Sternberg, A., Gal-Yam, A., Simon, J. D., et al. 2011, Science, 333, 856  
 Taam, R. E. 1980, ApJ, 242, 749  
 Travaglio, C., Hillebrandt, W., Reinecke, M., & Thielemann, F.-K. 2004, A&A, 425, 1029  
 van Kerkwijk, M. H., Chang, P., & Justham, S. 2010, ApJ Lett., 722, L157  
 Wang, B., & Han, Z. 2012, New Astron. Rev., 56, 122  
 Webbink, R. F. 1984, ApJ, 277, 355  
 Yungelson, L. R., Livio, M., Tutukov, A. V., & Saffer, R. A. 1994, ApJ, 420, 336  
 Zorotovic, M., Schreiber, M. R., Gänsicke, B. T., et al. 2011, A&A, 536, L3

## APPENDIX A:

As mentioned in Section 2, we assume that when a non-degenerate star accretes from its companion,  $f_a = 0.5$ , i.e. 50% of the mass lost from the companion is accreted while the other 50% is lost from the binary (see sect. 3.4 of Belczynski et al. 2008). In nature, it is not clear how much mass may be lost/gained in such a configuration, and the assumed value (and variability) of  $f_a$  has an important impact on the evolutionary outcome (see the case study of Mennekens et al. 2010). More important than the fraction of mass that is accreted might be in what manner angular momentum is lost from the binary system during non-conservative mass transfer (see also Claeys et al., in preparation, for a comparison study of four population synthesis codes).

For the current study, we used the published results from the standard model of Ruiter et al. (2011) for which  $f_a = 0.5$  was assumed. However, to obtain a general idea of how much our results might change if a different  $f_a$  value had been used, we performed additional smaller-scale STARTRACK runs for  $f_a = 0$  and  $f_a = 1$ . We find that the relative frequency of CO+CO WD mergers is highest for the fully non-conservative case: 1.2 : 1 : 0.4 for a  $f_a$  fraction of 0, 0.5 and 1, respectively. For more massive WD mergers however, the trend changes. For CO+CO WD mergers with  $M_{\text{tot}} > 1.4M_{\odot}$ , the relative frequency is 0.8 : 1 : 0.3 and for mergers which meet the criteria  $\eta = 1.5$ ,  $m_p > 0.8 M_{\odot}$ , the relative frequency is 0.5 : 1 : 0.3.

Thus, assuming fully conservative mass transfer onto non-degenerate accretors ( $f_a = 1$ ) seems at face value to result in an overall decrease in the number of CO+CO WD mergers. Our test here shows that the overall rates for massive CO+CO mergers might decrease at most by a factor of 3, though for fully non-conservative mass transfer the overall CO+CO WD merger rate could increase by 20%. The trend found here is somewhat different than that found by Mennekens et al. (2010), however: one must be cautious and accept that full evolutionary calculations (including other stages of binary evolution) are needed to properly compute any relative change in our results, and such a parameter study is beyond the scope of this paper.

## APPENDIX B:

Here we give the necessary information to reconstruct the fit in Figure 4. The 2-component fit was constructed with the following equality:

$$M_{\text{bol}} = \sum_{n=0}^{n_{\text{max}}} a_n m_{\text{WD}}^n \quad (\text{B1})$$

where coefficients  $a_n$  for the two different mass regimes can be found in Table B1.

## APPENDIX C:

Since on average the most luminous SNe Ia are often found among relatively young stellar populations, while less luminous SNe Ia are found among older stellar populations (Sect. 5.2.1), we can explore how the shape of the violent WD merger peak brightness distribution changes as a function of delay time.

We split our WD mergers (from Fig. 5) into two age groups: delay times less than 1 Gyr and delay times greater than 1 Gyr. The corresponding peak brightness distributions for these ‘younger’ and

**Table B1.** Coefficients for the polynomial and linear fits in Figure 4.

$0.8 < m_{\text{WD}} < 1.15$	
$n$	$a_n$
0	2403.1822
1	-10943.254
2	19821.934
3	-17966.776
4	8140.1093
5	-1473.6569
$1.15 < m_{\text{WD}} < 1.4$	
$n$	$a_n$
0	-16.827815
1	-2.0807692

‘older’ SNe Ia are shown in Fig. C1 and Fig. C2, respectively. From the Figures, it is clear that the shapes of our theoretical brightness distributions (coloured lines) do not change very much as a function of age. Additionally, using a different time cut does not change the results much either, since both bright and dim violent mergers occur at early and late delay times (see Sect. 5.2).

We additionally compare our theoretical distributions to the two luminosity functions of Li et al. (2011) that are separated by Hubble type. Li et al. (2011) split their luminosity functions into two groups based on host galaxy morphology: SNe Ia that are found in elliptical galaxies and spiral galaxies of type Sa, and SNe Ia that are found in spiral galaxies of type Sb and irregular galaxies (see their fig. 5). While delay times for individual SNe are not available for the Li et al. (2011) sample, it is reasonable to assume that the average delay times for SNe Ia found among the group with elliptical galaxies will be larger than the average delay times for SNe Ia found in the group which contains irregular galaxies. This is reflected in the slightly higher proportion of low-luminosity events to high-luminosity events in Fig. C2 compared to Fig. C1 (greyscales). The Li et al. (2011) sample (both age groups) contains SNe with different spectral properties, and we have included all 74 objects regardless of their spectral classification (normal, high-velocity, 91T-like, 91bg-like, and 02cx-like).

We note finally that the comparison of the theoretical brightness distributions to the observational data is for illustrative purposes only, since an accurate comparison requires detailed information on the observed delay time distribution from the Li et al. (2011) sample. Furthermore, splitting the entire Li et al. (2011) sample as we have done increases statistical noise: some bins only contain one SN event (see fig. 5 of Li et al. (2011)). Despite these potential caveats, the overall distribution shapes (observed and theoretical) show similar trends, and compare relatively well. In any case, it is possible (even likely) that other formation channels and/or explosion mechanisms are also contributing at some level to the SN Ia population at early and/or late delay times (e.g. Kromer et al. 2012).

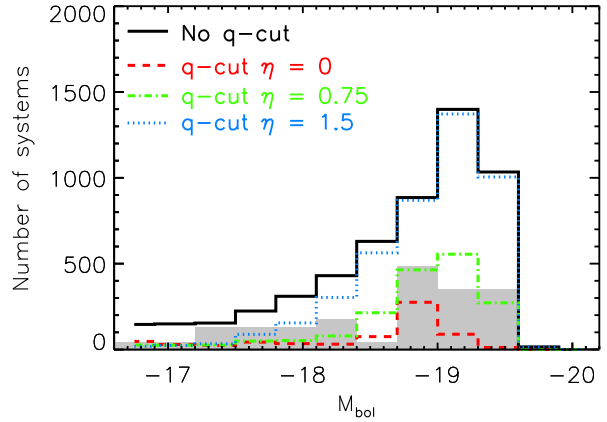


**Figure C1.** Greyscale shows the peak brightness distribution of SNe Ia from Sb spiral and irregular galaxies as shown in Li et al. (2011, fig. 5). Coloured lines show our theoretical peak brightness distributions for WD mergers with delay times less than 1 Gyr. Such a split enables all ‘prompt’ SNe Ia from violent mergers to be included in the distribution, while still including some SNe with intermediate delay times, which would be expected in an observed sample involving spiral hosts (the ‘Sb spiral & irregular’ distribution of Li et al. (2011)).

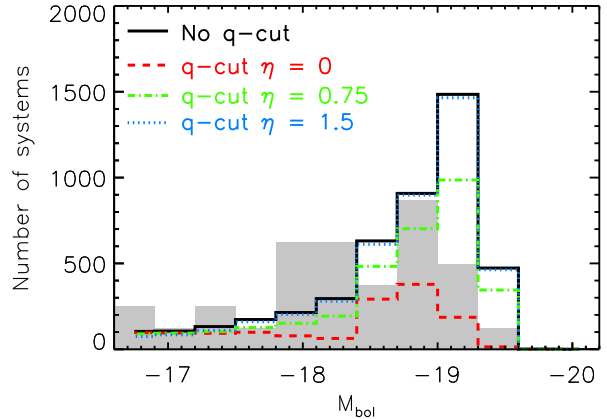


**Figure C2.** Greyscale shows the peak brightness distribution of SNe Ia from elliptical and Sa spiral galaxies as shown in Li et al. (2011, fig. 5). Coloured lines show our theoretical peak brightness distributions for WD mergers with delay times greater than 1 Gyr.